

Electronic Supplementary Information

Growing modulator agents for the synthesis of Al-MOF-type materials based on assembled 1D structural sub-domains

José María Moreno, Alexandra Velyt, José A. Vidal-Moya, Urbano Díaz* and Avelino Corma*

Instituto de Tecnología Química, Universitat Politècnica de València-Consejo Superior de Investigaciones Científicas, Avenida de los Naranjos s/n, E-46022 Valencia, Spain

E-mail: udiaz@itq.upv.es; acorma@itq.upv.es

Index

Table S1. Chemical analysis of 3D standard MIL-53(Al), MIL-53(Al)-EB and MIL-53(Al)-HB materials synthesized in water as solvent.

Table S2. Chemical analysis of Al-ITQ-EB, Al-ITQ-HB and Al-ITQ-DB materials synthesized in DMF solvent.

Table S3. Chemical analysis of L-MOF-EB, L-MOF-HB and L-MOF-DB materials synthesized in DMF-water mixtures as solvent.

Table S4. Yields and selectivity for 1,5-benzodiazepine production using Al-MOF-type materials as catalysts.

Scheme S1. Products of cylocondensation between acetone and o-phenylenediamine.

Figure S1. TEM images: (a) MIL-53(Al)-EB and (b) MIL-53(Al)-HB samples.

Figure S2. FESEM images: (a) and (b) 3D standard MIL-53(Al), (c) MIL-53(Al)-EB and (d) MIL-53(Al)-HB samples.

Figure S3. TEM images: (a) Al-ITQ-EB, (b) and (c) Al-ITQ-HB, and (d) Al-ITQ-DB samples.

Figure S4. TEM images: (a) and (b) L-MOF-EB, (c) L-MOF-HB and (d) L-MOF-DB samples.

Figure S5. TEM images: (a) and (b) MIL-53(Al)-EB samples exfoliated by diethyl ether solution; (c) Al-ITQ-EB and (b) Al-ITQ-HB samples exfoliated by dichloromethane solution; (e) L-MOF-EB and (f) L-MOF-DB samples exfoliated by diethyl ether solution.

Figure S6. TG and DTA curves: (a) 3D standard MIL-53(Al), (b) MIL-53(Al)-EB and (c) MIL-53(Al)-HB.

Figure S7. TG and DTA curves: (a) Al-ITQ-EB, (b) Al-ITQ-HB and (c) Al-ITQ-DB.

Figure S8. TG and DTA curves: (a) L-MOF-EB, (b) L-MOF-HB and (c) L-MOF-DB.

Figure S9. XRD patterns of MIL-53(Al)-HB materials: (a) as-synthesized, (b) 200°C, (c), 300°C and (d) 400°C.

Figure S10. XRD patterns of L-MOF-HB materials: (a) as-synthesized, (b) 200°C, (c), 250°C, (d) 300°C, (e) 350°C and (f) 400°C.

Figure S11. IR spectra: (a) 3D standard MIL-53(Al), (b) MIL-53(Al)-EB and (c) MIL-53(Al)-HB.

Figure S12. IR spectra: (a) Al-ITQ-EB, (b) Al-ITQ-HB and (c) Al-ITQ-DB.

Figure S13. IR spectra: (a) L-MOF-EB, (b) L-MOF-HB and (c) L-MOF-DB.

Figure S14. Difference FTIR spectra of increasing amounts of CO adsorbed at low temperature (100 K) on 3D standard MIL-53(Al) (self-supporting wafer).

Figure S15. Difference FTIR spectra of increasing amounts of CO adsorbed at low temperature (100 K) on MIL-53(Al)-HB sample (self-supporting wafer).

Figure S16. Difference FTIR spectra of increasing amounts of CO adsorbed at low temperature (100 K) on Al-ITQ-HB sample (MOF-type:SiO₂ 1.5:1 wafer).

Figure S17. Difference FTIR spectra of increasing amounts of CO adsorbed at low temperature (100 K) on L-ITQ-EB sample (self-supporting wafer).

Figure S18. Argon adsorption isotherms: (a) MIL-53(Al)-HB, (b) L-MOF-HB and (c) Al-ITQ-HB.

Figure S19. Hörvath-Kawazoe pore size distribution obtained from Ar adsorption isotherms: (a) MIL-53(Al)-HB, (b) L-MOF-HB and (c) Al-ITQ-HB.

Figure S20. XRD patterns of Al-ITQ-HB sample: (a) fresh and (b) first use.

Figure S21. XRD patterns of MIL-53(Al)-HB catalyst: (a) fresh, (b) first use, (c) second use, (d) third use and (e) fourth use.

Figure S22. ¹³C MAS NMR spectra of MIL-53(Al)-HB sample: (a) fresh and (b) fourth use.

Tables

Table S1. Chemical analysis of 3D standard MIL-53(Al), MIL-53(Al)-EB and MIL-53(Al)-HB materials synthesized in water as solvent.

Samples	Org.Cont. ^a					
	C ^a	H ^a	N ^a	CHN ^b	TGA ^c	Al ^a
MIL-53(Al)	43.5	2.4	0	45.9	70.2	13.8
MIL-53(Al)-EB	42.3	2.9	0.5	45.7	68.6	11.3
MIL-53(Al)-HB	41.8	4.1	0.3	46.2	69.5	7.6

^a Percentage in weight (%wt). ^b Organic content from CHNS elemental analysis. ^c Organic content from thermogravimetical analysis without taking account hydration water.

Table S2. Chemical analysis of Al-ITQ-EB, Al-ITQ-HB and Al-ITQ-DB materials synthesized in DMF solvent.

Samples	Org.Cont. ^a					
	C ^a	H ^a	N ^a	CHN ^b	TGA ^c	Al ^a
Al-ITQ-EB	21.9	3.9	0	25.8	38.1	27.8
Al-ITQ-HB	34.4	5.6	0.3	40.3	54.1	11.1
Al-ITQ-DB	44.3	7.4	0	51.7	61.0	17.3

^a Percentage in weight (%wt). ^b Organic content from CHNS elemental analysis. ^c Organic content from thermogravimetical analysis without taking account hydration water.

Table S3. Chemical analysis of L-MOF-EB, L-MOF-HB and L-MOF-DB materials synthesized in DMF-water mixtures as solvent.

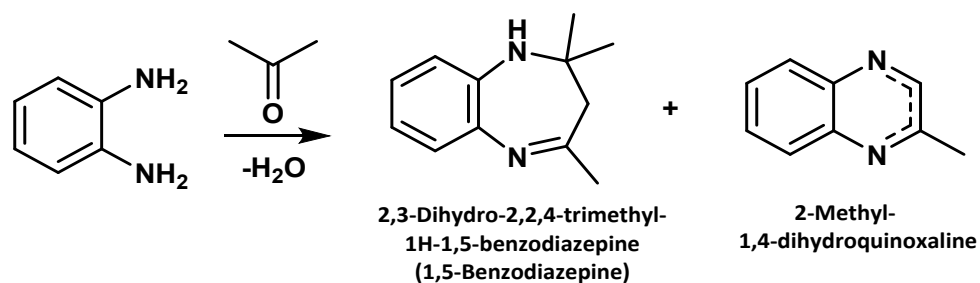
Samples	Org.Cont. ^a					
	C ^a	H ^a	N ^a	CHN ^b	TGA ^c	Al ^a
L-MOF-EB	61.5	5.6	0	67.1	84.4	9.0
L-MOF-HB	60.8	7.5	0	68.3	85.9	7.9
L-MOF-DB	64.4	9.0	0	73.4	83.8	6.9

^a Percentage in weight (%wt). ^b Organic content from CHNS elemental analysis. ^c Organic content from thermogravimetical analysis without taking account hydration water.

Table S4. Yields and selectivity for 1,5-benzodiazepine production^a.

Catalysts	Yield of 1,5-Benzodiazepines [%]	Yield of Imine [%]	Yield Subproduct [%] ^b	Selectivity [%]
MIL-53(Al)-EB	96	2	1	97
MIL-53(Al)-HB	90	4	6	90
L-MOF-EB	46	35	4	54
L-MOF-HB	68	16	16	68
L-MOF-DB	76	15	7	78

^a Reaction conditions: Diamine (0.5 mmol), acetone (10 mmol), 14 mol %Al, at 65°C, 10 h; ^b 2-Methyl-1,4-dihydroquinoxaline.



Scheme S1. Products of cylocondensation between acetone and o-phenylenediamine

Figures

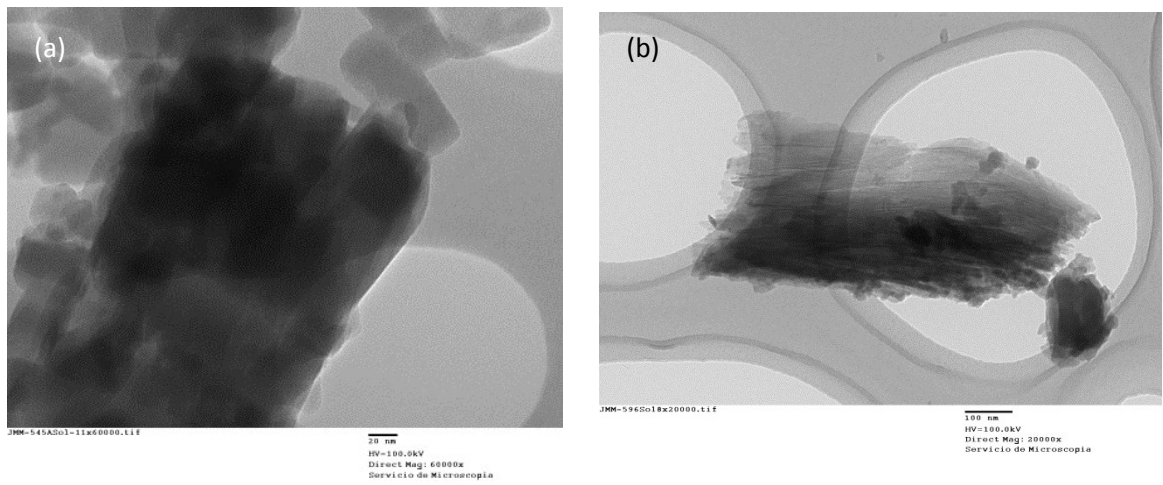


Figure S1. TEM images: (a) MIL-53(Al)-EB and (b) MIL-53(Al)-HB samples. Scale bars correspond to 20 nm and 100 nm for (a) and (b) images, respectively.

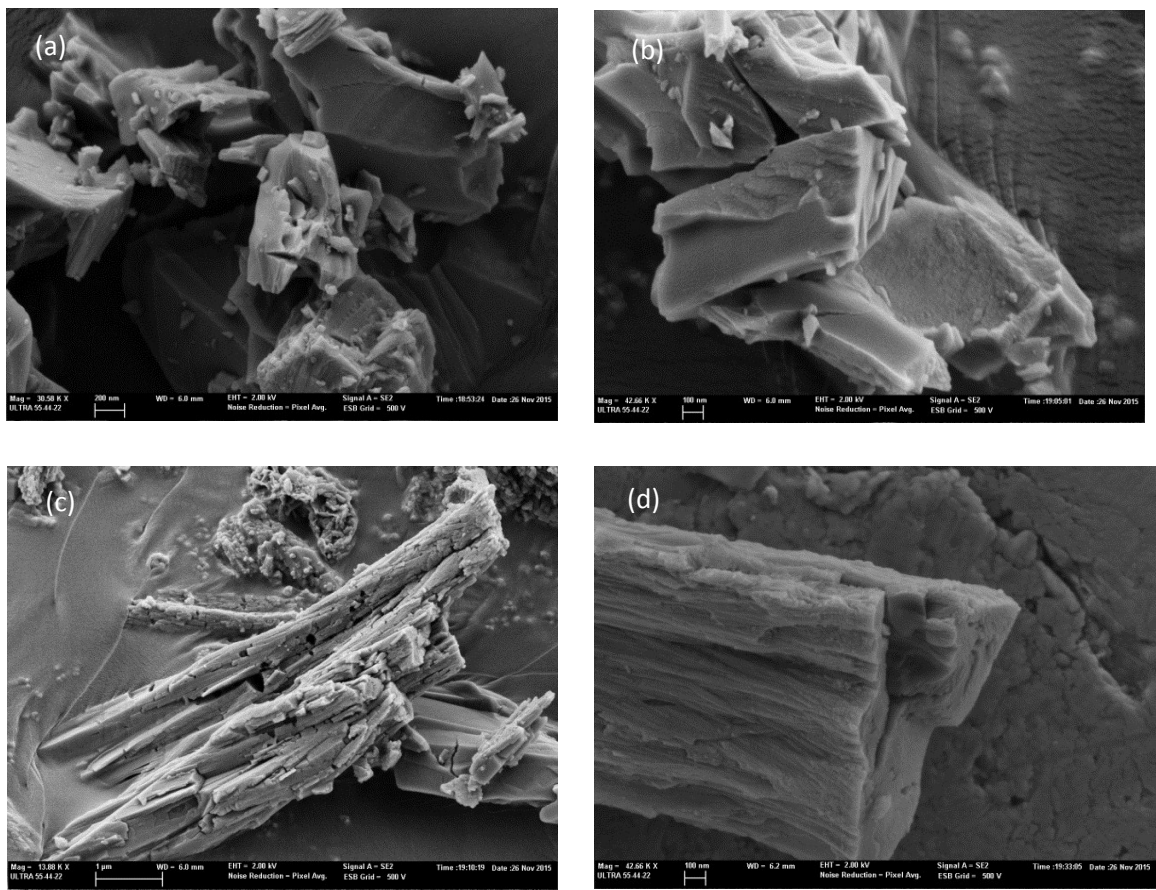


Figure S2. FESEM images: (a) and (b) 3D standard MIL-53(Al), (c) MIL-53(Al)-EB and (d) MIL-53(Al)-HB samples. Scale bars correspond to 200 nm, 100 nm, 1μm and 100 nm for (a), (b), (c) and (d) images, respectively.

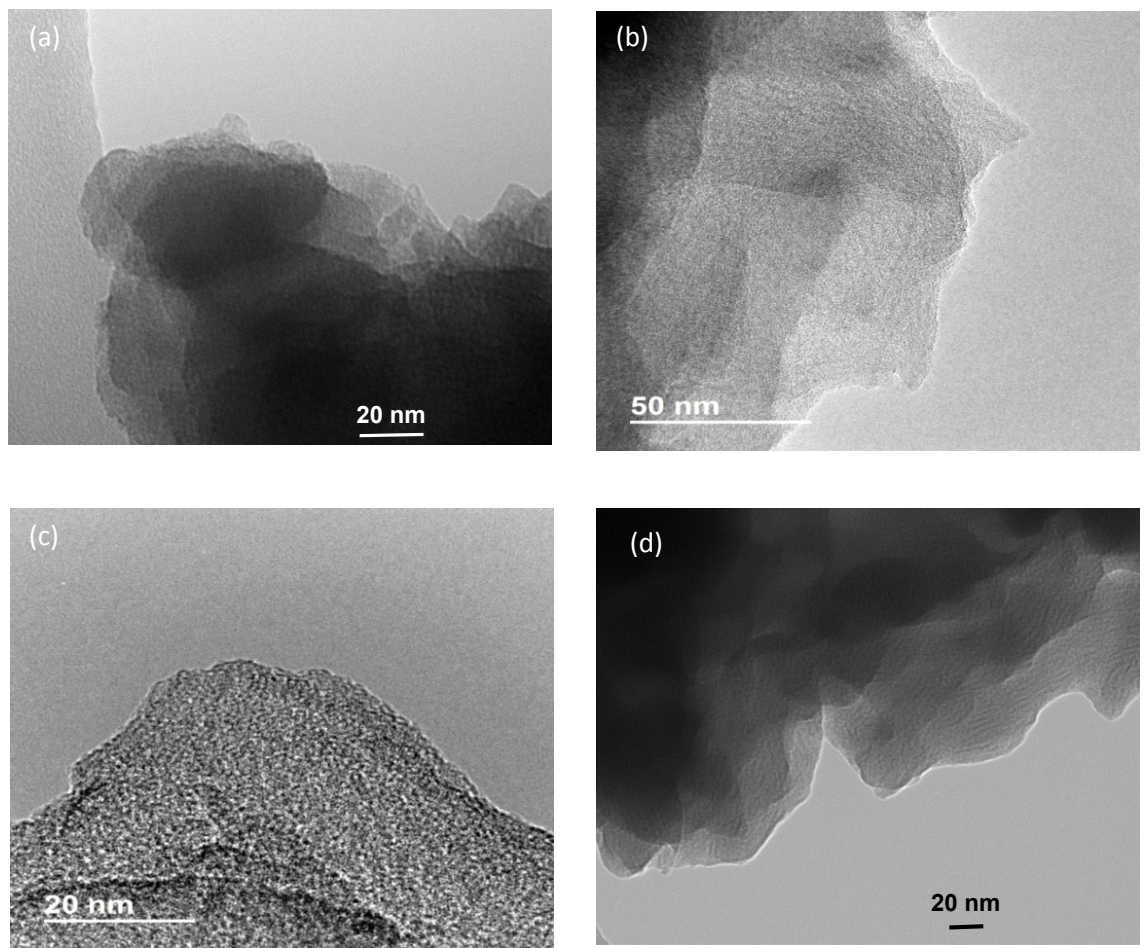


Figure S3. TEM images: (a) Al-ITQ-EB, (b) and (c) Al-ITQ-HB, and (d) Al-ITQ-DB samples. Scale bars correspond to 20 nm for (a), (c) and (d) micrographs, and 50 nm for (b) micrograph.

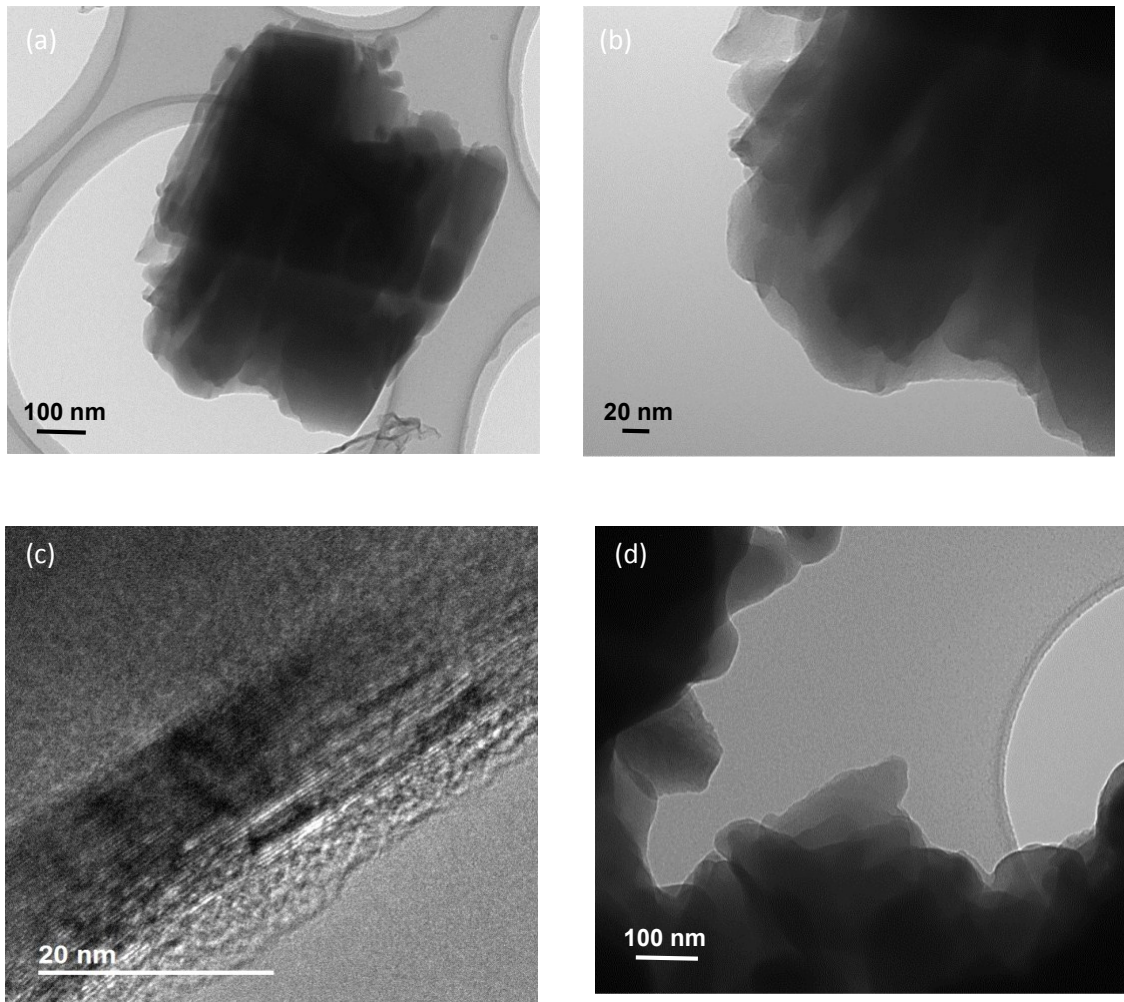


Figure S4. TEM images: (a) and (b) L-MOF-EB, (c) L-MOF-HB and (d) L-MOF-DB samples. Scale bars correspond to 100 nm for (a) and (d) micrographs, and 20 nm for (b) and (c) micrographs.

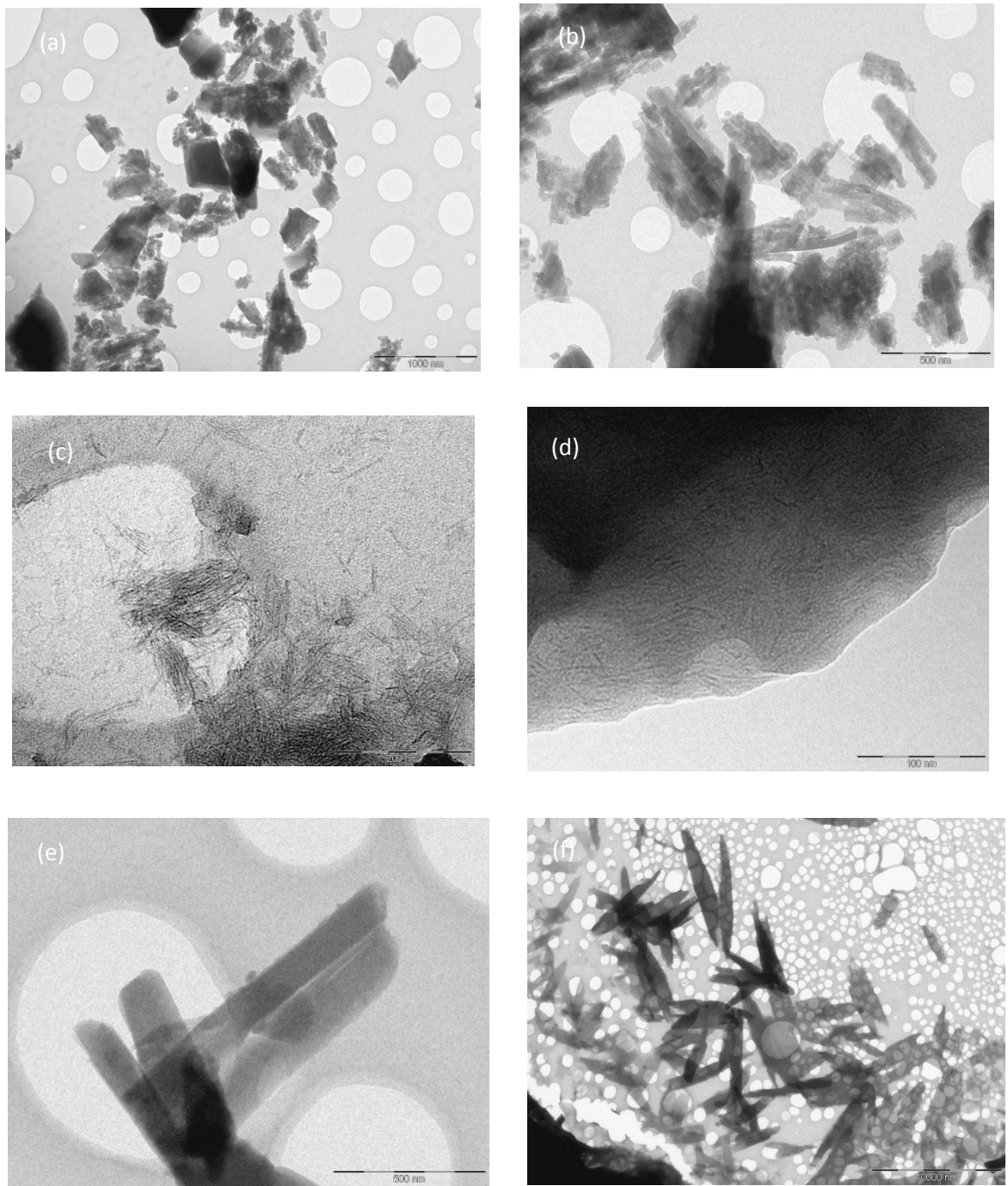


Figure S5. TEM images: (a) and (b) MIL-53(Al)-EB samples exfoliated by diethyl ether solution; (c) Al-ITQ-EB and (d) Al-ITQ-HB samples exfoliated by dichloromethane solution; (e) L-MOF-EB and (f) L-MOF-DB samples exfoliated by diethyl ether solution. Scale bars correspond to 1 μm , 500 nm, 200 nm, 100 nm, 500 nm and 1 μm for (a), (b), (c), (d), (e) and (f) samples, respectively.

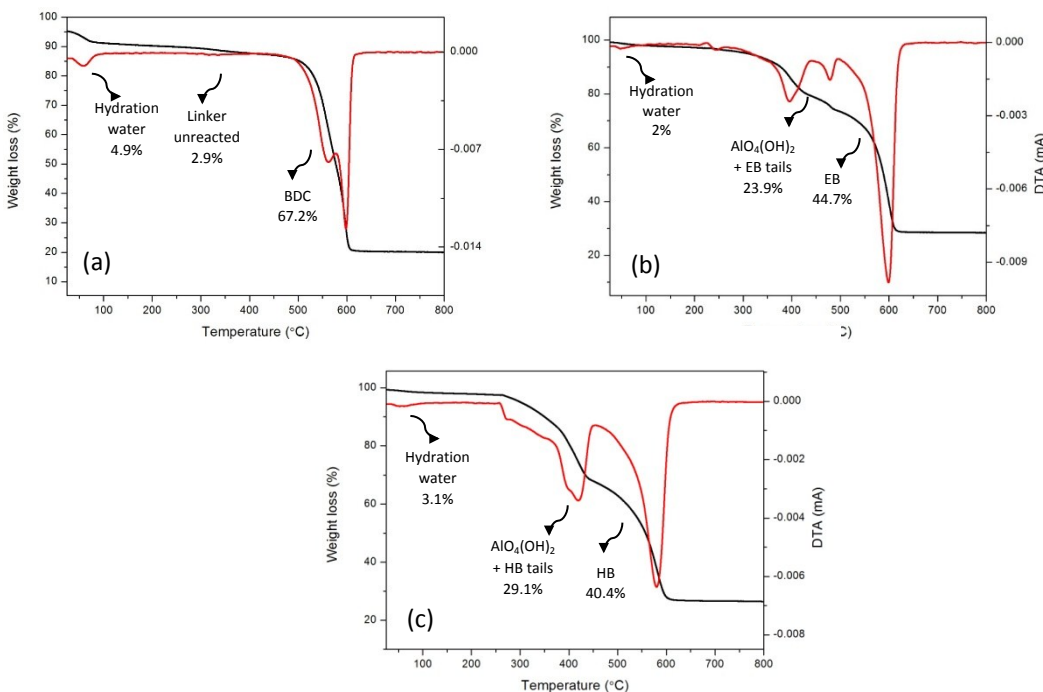


Figure S6. TG and DTA curves: (a) 3D standard MIL-53(Al), (b) MIL-53(Al)-EB and (c) MIL-53(Al)-HB.

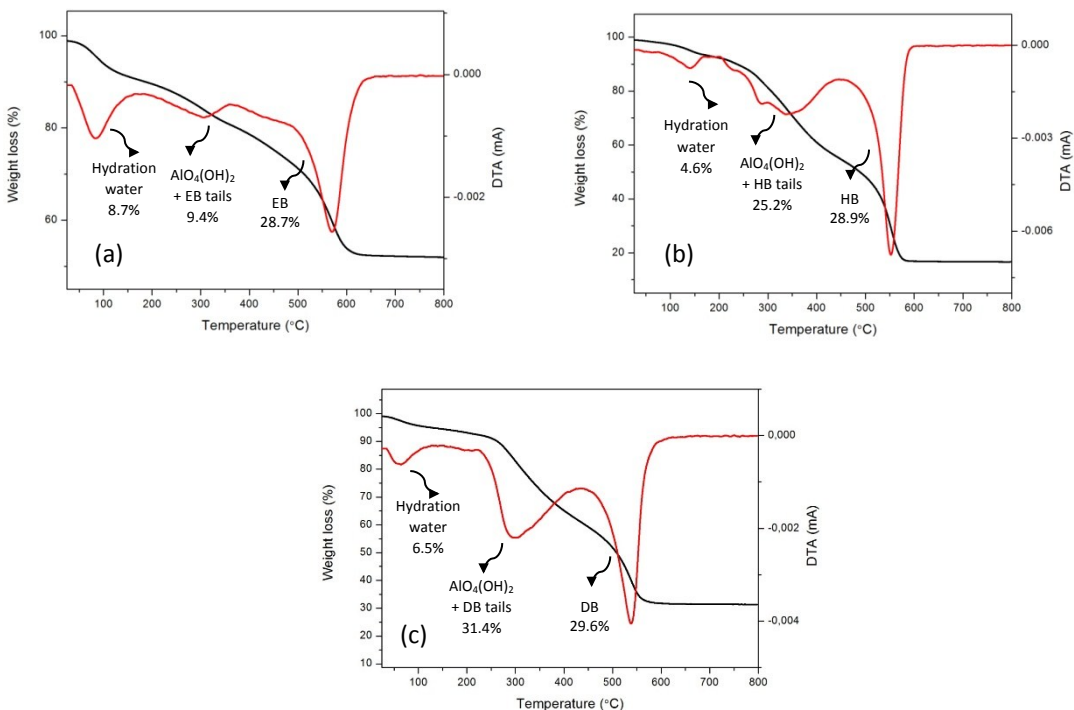


Figure S7. TG and DTA curves: (a) Al-ITQ-EB, (b) Al-ITQ-HB and (c) Al-ITQ-DB.

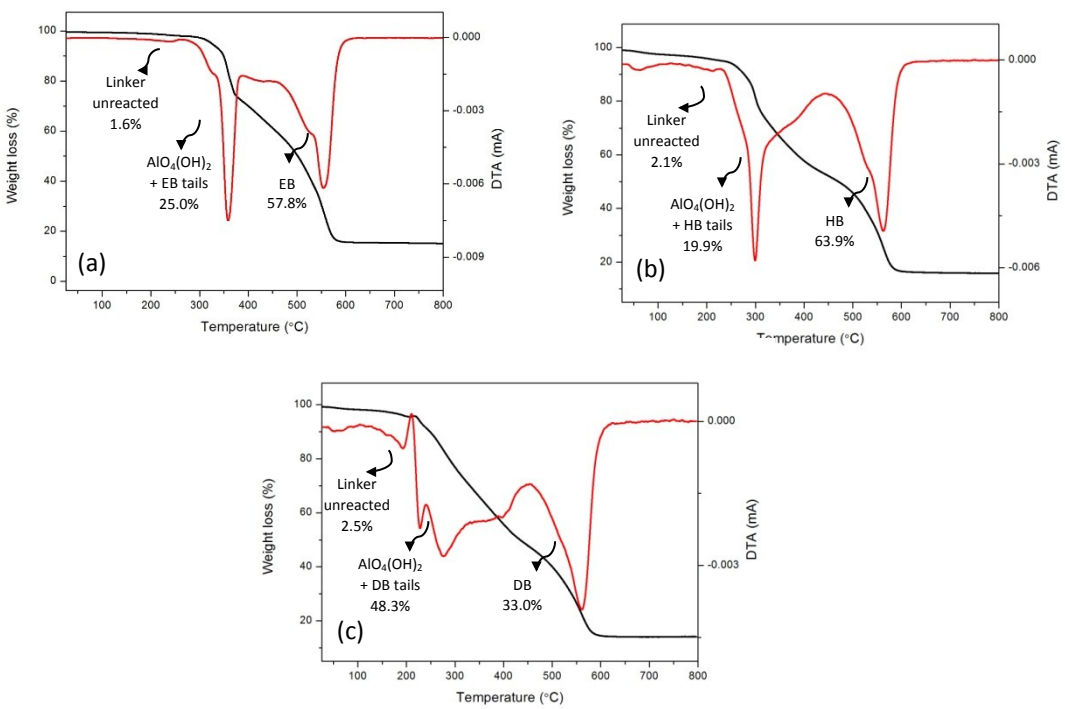


Figure S8. TG and DTA curves: (a) L-MOF-EB, (b) L-MOF-HB and (c) L-MOF-DB.

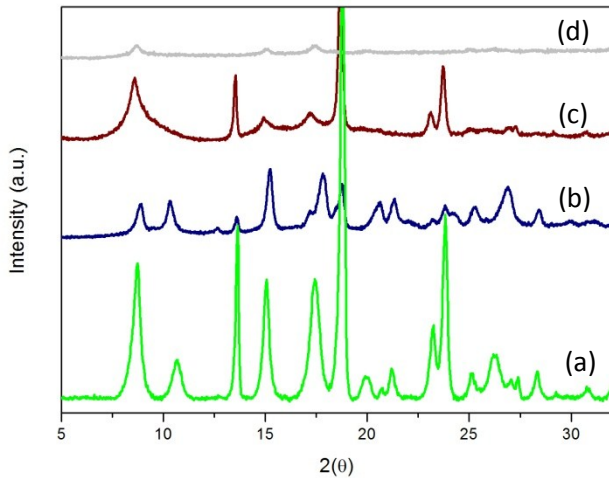


Figure S9. XRD patterns of MIL-53(Al)-HB materials: (a) as-synthesized, (b) 200 $^{\circ}\text{C}$, (c), 300 $^{\circ}\text{C}$ and (d) 400 $^{\circ}\text{C}$.

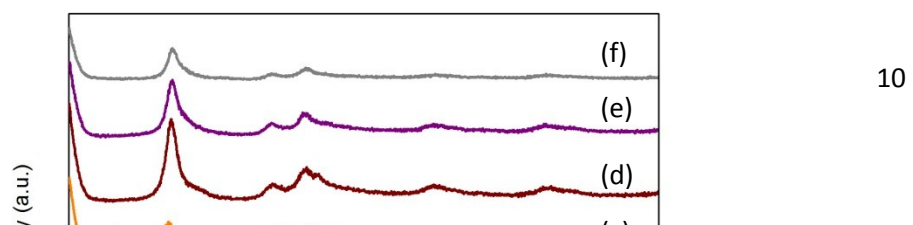


Figure S10. XRD patterns of L-MOF-HB materials: (a) as-synthesized, (b) 200°C, (c), 250°C, (d) 300°C, (e)350°C and (f) 400°C.

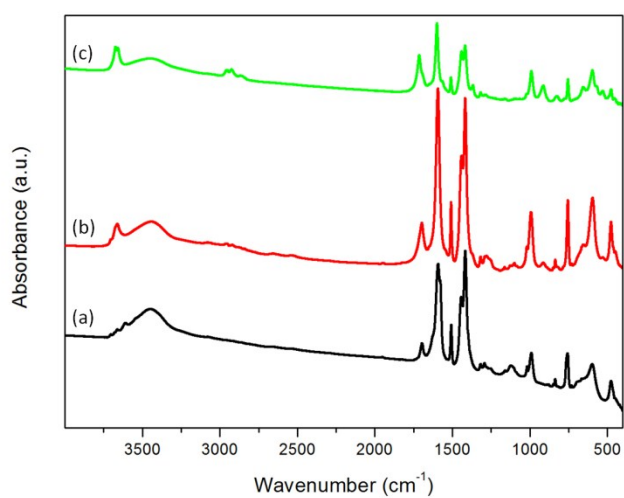


Figure S11. IR spectra: (a) 3D standard MIL-53(Al), (b) MIL-53(Al)-EB and (c) MIL-53(Al)-HB.

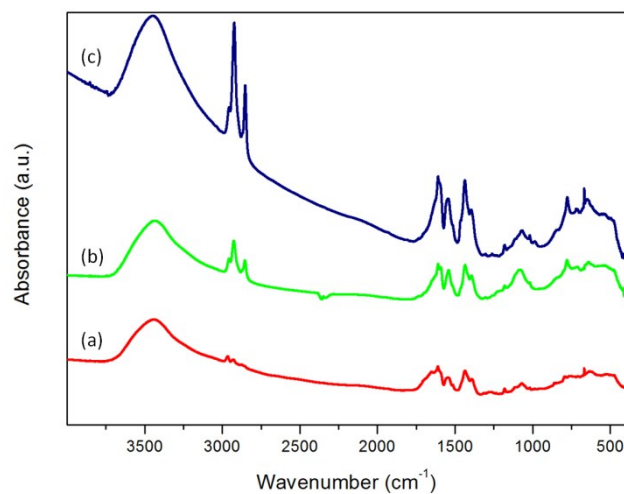


Figure S12. IR spectra: (a) Al-ITQ-EB, (b) Al-ITQ-HB and (c) Al-ITQ-DB.

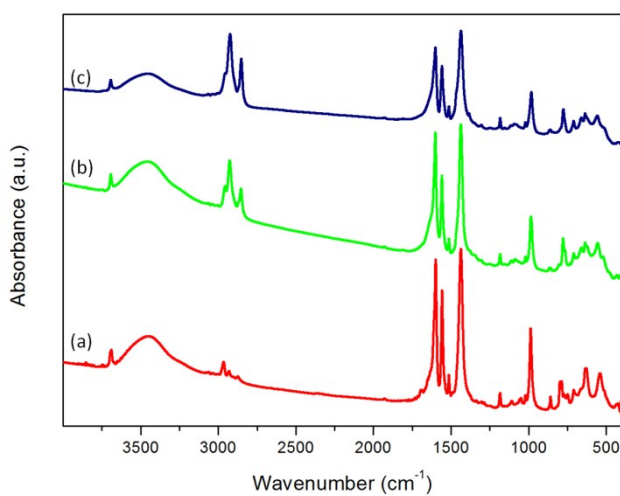


Figure S13. IR spectra: (a) L-MOF-EB, (b) L-MOF-HB and (c) L-MOF-DB.

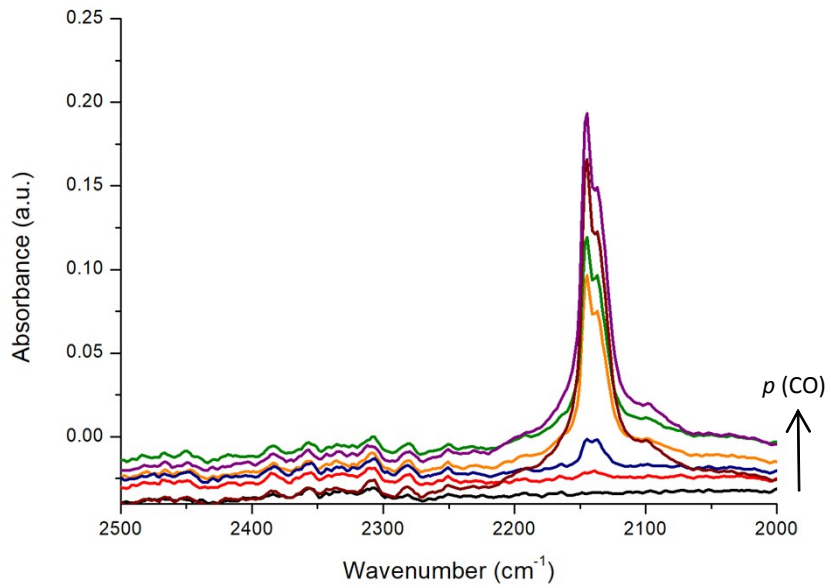


Figure S14. Difference FTIR spectra of increasing amounts of CO adsorbed at low temperature (100 K) on 3D standard MIL-53 (Al) (self-supporting wafer).

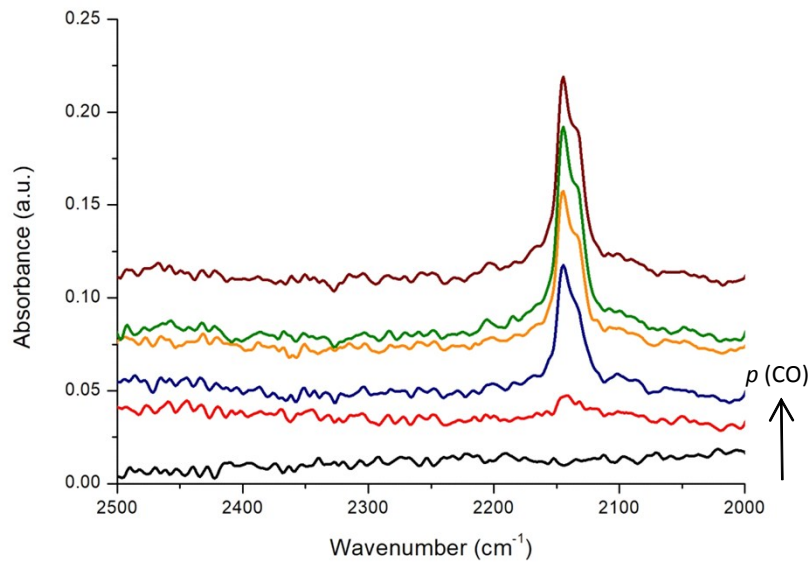


Figure S15. Difference FTIR spectra of increasing amounts of CO adsorbed at low temperature (100 K) on MIL-53(Al)-HB sample (self-supporting wafer).

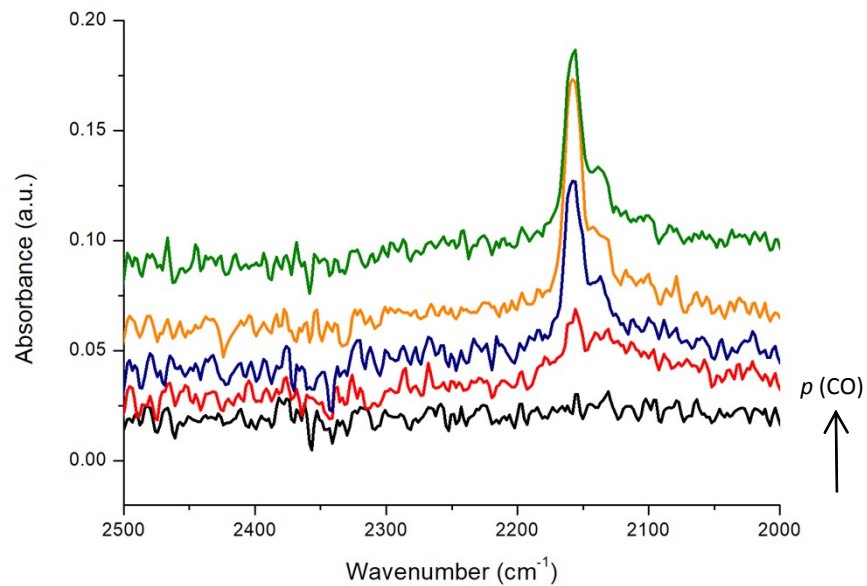


Figure S16. Difference FTIR spectra of increasing amounts of CO adsorbed at low temperature (100 K) on Al-ITQ-HB sample (MOF-type:SiO₂ 1.5:1 wafer).

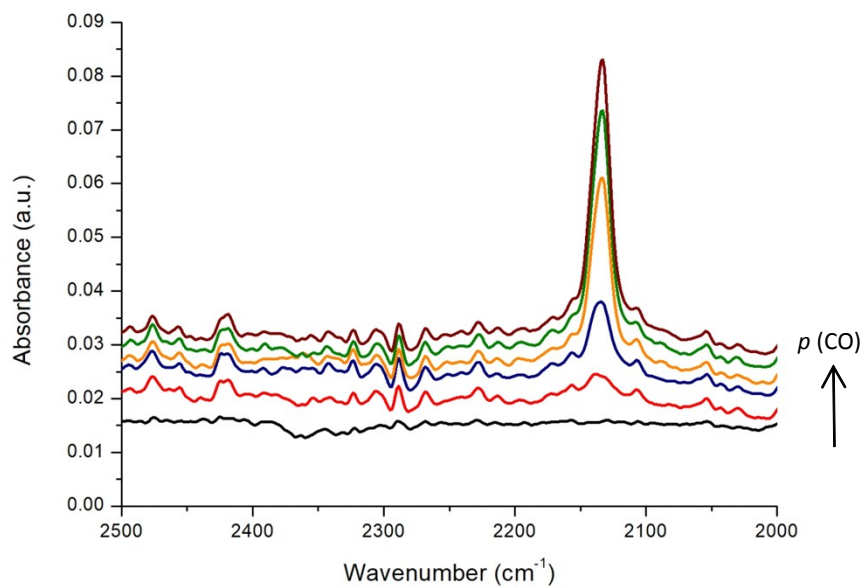


Figure S17. Difference FTIR spectra of increasing amounts of CO adsorbed at low temperature (100 K) on L-ITQ-EB sample (self-supporting wafer).

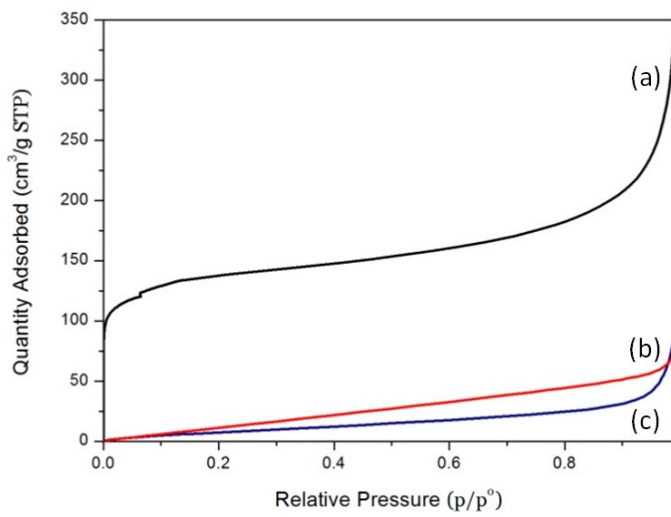


Figure S18. Argon adsorption isotherms: (a) MIL-53(Al)-HB, (b) L-MOF-HB and (c) Al-ITQ-HB.

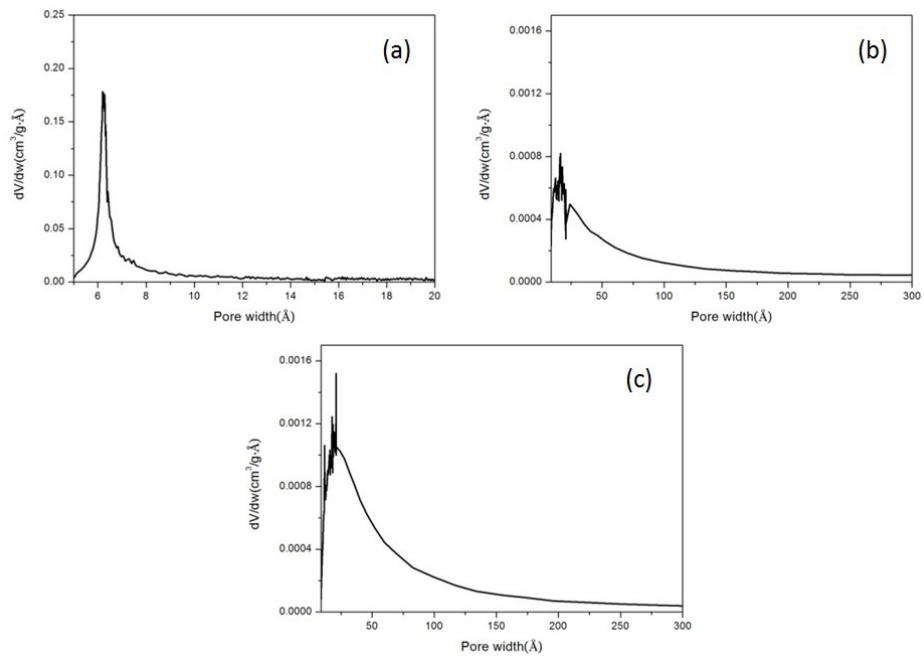


Figure S19. Hörvath-Kawazoe pore size distribution obtained from Ar adsorption isotherms: (a) MIL-53(Al)-HB, (b) L-MOF-HB and (c) Al-ITQ-HB.

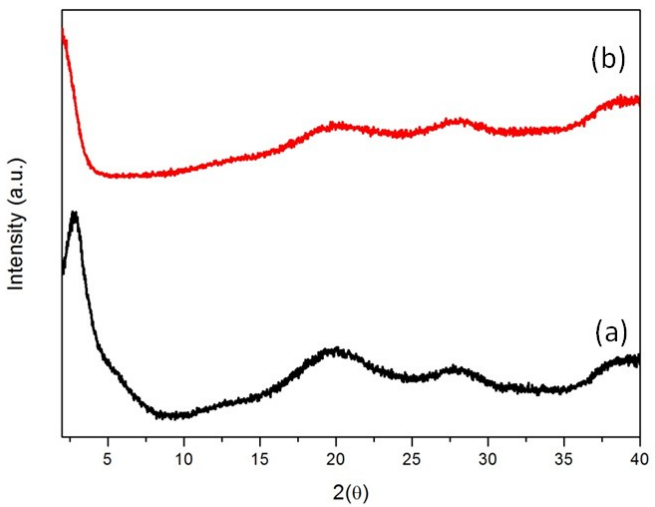


Figure S20. XRD patterns of Al-ITQ-HB sample: (a) fresh and (b) first use.

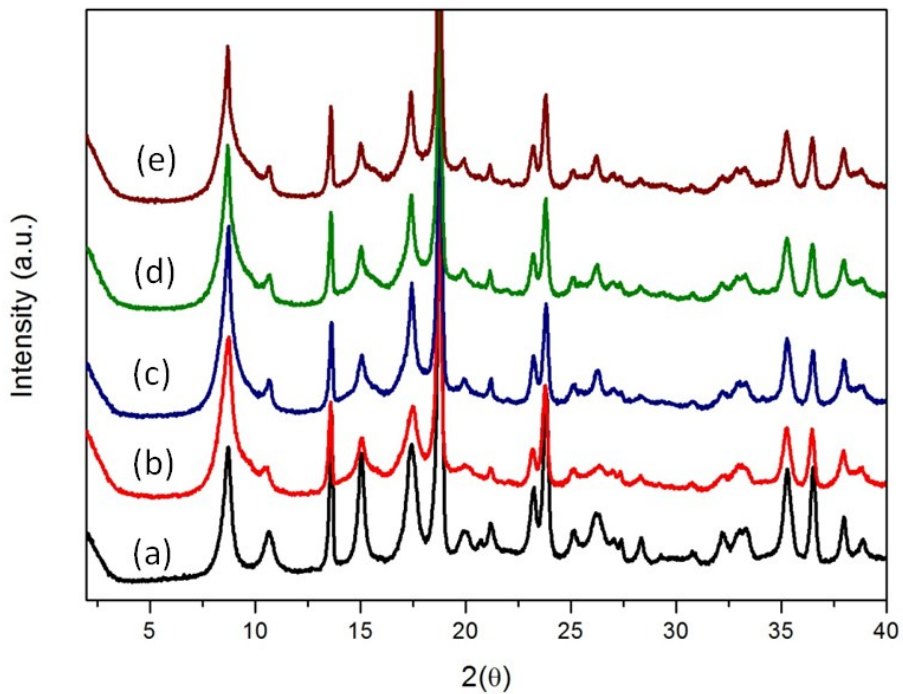


Figure S21. XRD patterns of MIL-53(Al)-HB catalyst: (a) fresh, (b) first use, (c) second use, (d) third use and (e) fourth use.

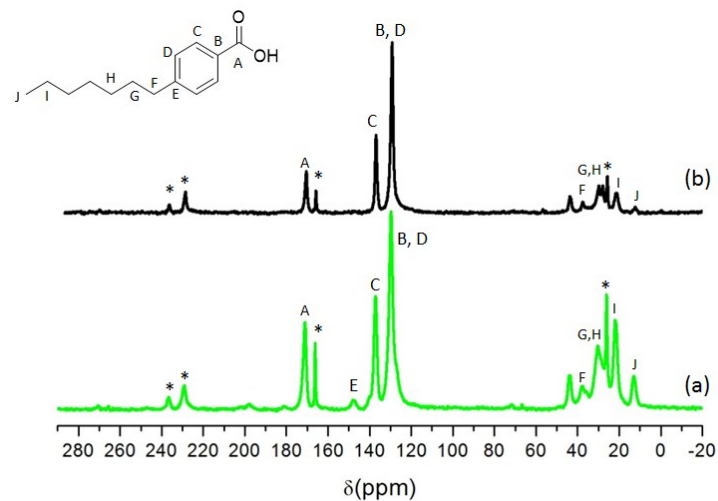


Figure S22. ¹³C MAS NMR spectra of MIL-53(Al)-HB sample: (a) fresh and (b) fourth use.